ACS APPLIED MATERIALS & INTERFACES

Research Article

www.acsami.org

A Delicate Balance When Substituting a Small Hydrophobe onto Low Molecular Weight Polyethylenimine to Improve Its Nucleic Acid Delivery Efficiency

Deniz Meneksedag-Erol,[†,‡] Remant Bahadur KC,[‡] Tian Tang,[*,†,§] and Hasan Uludağ[*,†,‡,∥]

[†]Department of Biomedical Engineering, Faculties of Medicine & Dentistry and Engineering, [‡]Department of Chemical & Materials Engineering, Faculty of Engineering, [§]Department of Mechanical Engineering, Faculty of Engineering, and [∥]Faculty of Pharmacy and Pharmaceutical Sciences, University of Alberta, Alberta, Canada

Supporting Information

ABSTRACT: High molecular weight (HMW) polyethylenimine (PEI) is one of the most versatile nonviral gene vectors that was extensively investigated over the past two decades. The cytotoxic profile of HMW PEI, however, encouraged a search for safer alternatives. Because of lack of cytotoxicity of low molecular weight (LMW) PEI, enhancing its performance via hydrophobic modifications has been pursued to this end. Since the performance of modified PEIs depends on the nature and extent of substituents, we systematically investigated the effect of hydrophobic modification of LMW (1.2 kDa) PEI with a short propionic acid (PrA). Moderate enhancements in PEI hydrophobicity resulted in enhanced cellular uptake of polyplexes and siRNA-induced silencing efficacy, whereas further increase in PrA substitution abolished the uptake as well as the silencing. We performed all-atom molecular dynamics simulations to elucidate the mechanistic details behind these observations. A new assembly mechanism was observed by the presence of hydrophobic PrA moieties, where PrA migrated to core of the polyplex. This phenomenon caused higher surface hydrophobicity and surface charge density at low substitutions, and it caused deleterious effects on surface hydrophobicity and cationic charge at higher substitutions. It is evident that an optimal balance of hydrophobicity/hydrophilicity is needed to achieve the desired polyplex properties for an efficient siRNA delivery, and our mechanistic findings should provide valuable insights for the design of improved substituents on nonviral carriers.

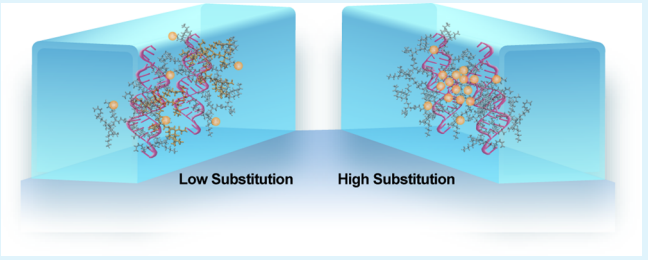

KEYWORDS: *siRNA, polyethylenimine, hydrophobic modification, gene delivery, molecular dynamics*

1. INTRODUCTION

Delivery of genetic material, either DNA or RNA, into cells and tissues to cope with defective physiology has proven to be a promising alternative in treating genetic disorders and cancers.[1] Silencing aberrant gene expression with synthetic double-stranded short interfering RNAs (siRNAs), in particular, has gained attention since Fire and co-workers[2] revealed the concept of RNA interference (RNAi) in nematode *Caenorhabditis elegans*. Successful delivery of siRNA into the targeted cells is of vital importance in the suppression of abnormal gene expression at therapeutic level. Susceptibility of nucleic acids to serum nucleases, however, hindered the delivery of naked siRNAs and led to the requirement of a delivery system in therapeutic applications. An efficient delivery system should facilitate the targeting of siRNAs to desired cells and tissues with minimal off-site effects, protect the siRNAs from nucleases, promote the cellular uptake of the cargo by endocytosis, and facilitate its intracellular trafficking.[1] Nonviral carriers have acquired considerable attention in this context, due to their relatively safe and easy-to-engineer nature in comparison to their viral counterparts.

Polyethylenimine (PEI) is a polymeric carrier that displays beneficial properties especially in the endosomal stages of delivery, hypothesized to originate from its uncharged nitrogens acting as a proton sponge to delay acidification in the endocytic vesicles.[3,4] It has been tested extensively for its gene delivery performance in a number of cell lines.[5] Its efficacy in transfecting DNA was found to increase with its molecular weight;[6,7] however, high molecular weight (HMW) PEIs possess a considerable amount of toxicity, by inducing damage to the plasma membrane hence causing loss of metabolic activity.[7,8] In search for a safer, nontoxic, and nonimmunogenic alternative to HMW PEI, research has focused on improving the performance of nontoxic low molecular weight (LMW) PEI via various modifications.

Polyplexes must translocate through a lipid-based plasma membrane, where they are expected to preserve their integrity to effectively deliver their cargo to the cell interior.[9] Modification of carriers with hydrophobic moieties may

Received: August 25, 2015
Accepted: October 23, 2015
Published: October 23, 2015

DOI: 10.1021/acsami.5b07929
ACS Appl. Mater. Interfaces 2015, 7, 24822−24832

facilitate the entry to cells by promoting hydrophobic interactions with membrane lipids.[10] Improvements in LMW PEI's gene delivery efficacy were reported with substitution of various hydrophobic molecules, including bulky hydrophobe groups such as cholesterol[11−13] and phospholipids such as phosphoethanolamine (DOPE and DPPE) and phosphocholine (PC),[14] which yielded enhanced transfection and/or silencing efficacy. Modification of 1.8 kDa PEI with hydrophobic alkyl groups such as ethyl, octyl, and deodecyl induced higher transfection efficiencies than that of unmodified PEI.[14] Toward this end, aliphatic lipids were also investigated. A previous study from our group explored a variety of aliphatic substituents, such as caprylic (8C), myristic (14C), palmitic (16C), stearic (18C), oleic (18C with a double bond), and linoleic acid (18C with two double bonds). Regardless of the type of the engrafted substituent, performance of 2 kDa PEI was increased in transfecting the genes compared to its unmodified counterpart, and the efficacy of the modified polymers were comparable to HMW 25 kDa PEI.[9]

In this study, to have a better control over the grafting reactions, we explored the beneficial effect of a short aliphatic substituent, propionic acid (PrA, 3C), on the transfection ability of 1.2 kDa PEI. PrA moieties were grafted onto PEI at different substitution amounts, and siRNA delivery capability of the PrA-modified PEIs was systematically assessed in K562 cell line, a chronic myeloid leukemia (CML) model. Surprisingly, a nonmonotonic trend was observed between the uptake and gene silencing capability of the polyplexes and the amount of PrA substitution, with intermediate substitution amounts yielding the highest efficacy. To elucidate the molecular-level details behind this unexpected phenomenon, molecular dynamics (MD) simulations were performed on the designed polyplexes, and we proposed a molecular basis for the unexpected performance of the engineered polymers.

2. METHODS

2.1. Experimental Section. *Materials.* Branched 25 kDa PEI, PrA, *N*-(3-(dimethylamino)propyl)-*N*′-ethylcarbodiimide hydrochloride (EDC), *N*-hydroxysuccinimide (NHS) were obtained from Sigma-Aldrich (St. Louis, MO). Branched 1.2 kDa PEI was purchased from Polysciences, Inc. (Warrington, PA). Roswell Park Memorial Institute (RPMI) medium containing L-glutamine, 25 mM 4-(2-hydroxyethyl)-1-piperazineethanesulfonic acid (HEPES), penicillin, and streptomycin was obtained from Gibco (Grand Island, NY). Custom-synthesized green fluorescent protein (GFP) siRNA (5′-GAACUUC-AGGGUCAGCUUGCCG-3′ and 3′-UACUUGAAGUCCCA-GUCGAACG-5′), and 5′-carboxyfluorescein (FAM)-labeled scrambled siRNA (5′-AACCAGUCGCAAACGCGACUGTT-3′ and 5′-TTUUGGUCAGCGUUUGCGCUGAC-5′) were obtained from Integrated DNA Technologies, Inc. (IDT; Coralville, IA). All solvents used in the synthesis procedure were obtained from Sigma-Aldrich and used without any further purification.

Synthesis and Characterization of PrA-Modified Polymers. Hydrophobic modification of PEI with PrA was performed via *N*-acylation (Figure 1a). Briefly, PrA (3.34 mM, in $CHCl_3$) was activated, with EDC (5 mM, in $CHCl_3$) for 30 min and then with NHS (5 mM, in MeOH), at room temperature. The activated PrA solutions were added dropwise to each PEI solution (3.34 mM in $CHCl_3$) and stirred overnight at room temperature. The crude products of PrA-substituted PEIs of the four PrA/PEI feed ratios (0.5, 1, 2, and 4 mol/mol) were precipitated (3×) in ice cold diethyl ether and dried under vacuum for 48 h. Structural compositions of PrA-substituted PEIs and the amount of PrA substitution (α) were elucidated through ^{1}H NMR spectroscopy (Bruker 300 MHz, Billerica, MA) using tetramethylsilane as an internal standard in D_2O. Detailed information on the efficiency of the reactions and the characterization of the polymers is given in Section S1 of Supporting Information. Polymers will be referred to by their substitution amounts calculated from ^{1}H NMR spectrum given on the right column of Figure 1b.

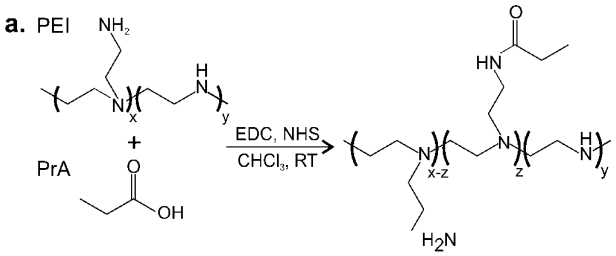

b.

Feed ratio PrA/PEI (mol/mol)	Calculated substitution amount (α) PrA/PEI (mol/mol)
0.50	0.26
1.00	0.69
2.00	1.14
4.00	1.59

Figure 1. (a) Scheme for the synthesis of PrA-conjugated PEIs. (b) Details on the synthesis of the polymers. The substitution amount (α) is calculated from ^{1}H NMR spectrum.

Cell Culture. Wild-type and permanently GFP-expressing K562 cells were used as the CML model. Cells were maintained in RPMI medium containing 10% fetal bovine serum (FBS), 100 U/ml penicillin, and 100 μg/mL streptomycin, and routinely grown on 75 cm^2 plates. Cells were passaged when they reached ∼80% confluence by simply dilution of the cell suspension by 1:10.

siRNA/Polymer Complex Preparation. For the preparation of siRNA/polymer complexes, 1.1 μg of siRNA was mixed with polymers (dissolved in ddH_2O) at polymer:siRNA weight ratio of 6:1, then incubated in 300 μL of RPMI (without FBS) for 30 min at room temperature. siRNA complexes (100 μL) were added to the cells in 48-well plates (in 300 μL of volume) in triplicate to give a final concentration of 60 nM siRNA in cell suspension.

Physicochemical Characterization of siRNA/Polymer Complexes. SiRNA/polymer complexes were prepared in 100 μL (total final volume) of ultrapure distilled H_2O by incubating 1.1 μg of scrambled siRNA with different amounts of polymers to achieve polymer:siRNA weight ratio of 6:1 for particle size and of 1:1, 3:1, and 6:1 for zeta (ζ) potential measurements. Hydrodynamic diameter and ζ-potential of the particles were investigated by dynamic light and electrophoretic light scattering methods using Zetasizer (Nano ZS; Malvern Instruments, UK). The measurements were performed at least in triplicate.

siRNA Delivery to K562 Cells. For cellular uptake studies, complexes were prepared with FAM-labeled scrambled siRNA with the procedure described above. K562 wild-type cells (300 μL, 100 000 cells/mL) were then added on top of the complexes in 48-well plates. Cells were incubated for 24 h at 37 °C in a humidified atmosphere. After incubation for a desired period, cells were processed for flow cytometry. Briefly, cells were transferred into 1.5 mL tubes and centrifuged at 1400 rpm for 5 min, washed twice with Hank's balanced salt solution (HBSS; pH 7.4), and fixed with formalin (3.7% in HBSS). FAM-siRNA positive cell population was quantified by Beckman Coulter QUANTA SC Flow Cytometer using FL1$^+$ channel (3000 events/sample). The setting of the instrument was calibrated for each run to obtain FAM-siRNA positive cell population of 1−2% for control samples (i.e., untreated cells). The mean fluorescence intensity (MFI) and the percentage of FAM-siRNA positive cells were determined.

GFP Silencing in GFP Positive K562 Cells. Silencing activity of the complexes was determined by quantifying the decrease in GFP fluorescence in GFP-expressing K562 cells. Complexes were prepared with GFP siRNA with the procedure described above, then GFP-expressing K562 cells were seeded on top of the complexes and grown for 72 h. For the first time point (day 3), 300 μL of the cells was transferred into 1.5 mL tubes and centrifuged at 1400 rpm for 5 min, washed twice with HBSS (pH 7.4), and fixed with formalin (3.7% in

DOI: 10.1021/acsami.5b07929
ACS Appl. Mater. Interfaces 2015, 7, 24822−24832

HBSS). The remaining 100 μL of the cells was mixed with 300 μL of fresh media and incubated for next time points (days 6 and 9). GFP silencing was quantified by flow cytometry using FL1$^-$ channel. The results were expressed as either mean GFP fluorescence after treatment or as percentage of cells displaying GFP silencing after the treatment, as determined by a shift from native GFP-expressing cell population.

Cytotoxicity of the siRNA/Polymer Complexes. In vitro cytotoxicity of the complexes was studied in K562 wild-type cells by 3-(4,5-dimethylthiazol-2-yl)-2,5-diphenyl-tetrazolium bromide (MTT) assay. First, complexes were prepared in Eppendorf tubes by incubating (in 300 μL of RPMI) 1 μg of siRNA with various amounts of polymers for the final polymer:siRNA weight ratios ranging from 1:1 to 40:1. Upon 30 min of incubation at room temperature, complexes were transferred to 48-well plates in triplicate. K562 wild-type cells were then added on top of the complexes (60 000 cells/well) and incubated for 72 h at 37 °C in a humidified atmosphere. After incubation for the desired period, MTT reagent was added to each well in final concentration of 1 mg/mL and further incubated for 2 h. Deposited formazan crystals were dissolved by replacing the medium with dimethyl sulfoxide (DMSO; 200 μL). Optical density was measured at λ = 570 nm by using universal microplate reader (ELx; Bio-Tech Instrument, Inc.). Cell viability was expressed as percentage relative to the viability of the cells without any treatment.

2.2. Computational Section. *Simulated Systems.* The simulated siRNA has the following sequence: sense strand: 5′-CGCCGA-AUUCAUUAAUUUATT-3′, antisense strand: 5′-UAAAUU-AAUGAAUUCGGCGGG-3′, capable of silencing myeloid cell leukemia 1 (Mcl-1) protein. The total charge of siRNA is −40 in the fully deprotonated state. Its initial structure is created with UCSF Chimera[15] to be in canonical A-form. The 3′-overhangs were created with the manipulation of the structure via the mutation and/or deletion of the terminal bases. The simulated native PEI is branched and has a molecular weight of 1205 Da. Its chemical structure is given in Figure 2. It consists of 27 primary, secondary, or tertiary amine

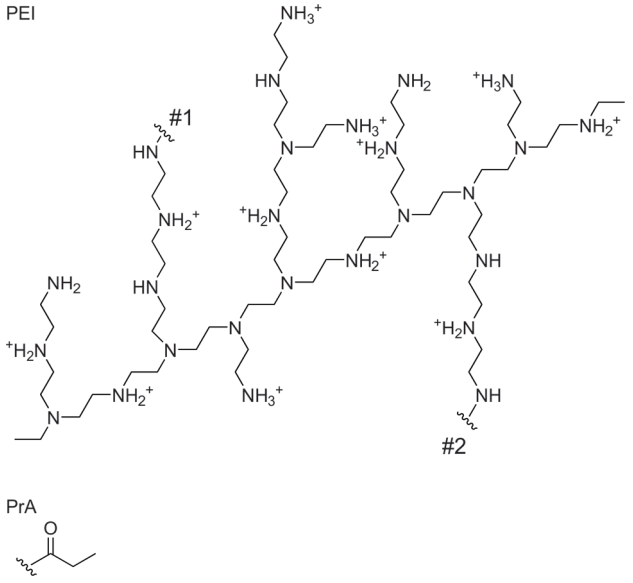

Figure 2. Molecular structures of the simulated PEI and PrA. (+) Protonation sites of PEI. (#) PrA substitution sites.

groups, of which 12 are protonated (indicated with (+) in Figure 2) corresponding to the protonation ratio of 44.4%, which is close to the experimentally determined ratio at pH = 6.[16] The protonation sites were assigned to primary and secondary amines and were distributed in a way to minimize the nonspecific attractions between protonated amine groups.[17] For the substitution of hydrophobic moieties into PEI's structure, two ratios were chosen: PEI-1PrA with one PrA molecule per PEI and PEI-2PrA with two PrA molecules per PEI. In PEI-1PrA, PrA is substituted into the structure of PEI at the site marked as #1, and in PEI-2PrA, two PrAs were substituted at sites #1 and #2 (Figure 2). Initial structures of the native and modified PEIs were built in Maestro 9.8[18] and VMD[19] software and equilibrated for 10 ns (restrained) + 10 ns (free) with MD package of NAMD.[20] The structures of the polymers at the end of the simulations were adopted as initial structures for the main simulations.

To explore the effect of hydrophobic modification, five simulation systems were then designed with varying PrA substitution amounts. To be consistent with the Experimental Section, simulated systems will be referred to by the amount of PrA substitution (α) they carry. Each system consists of 4 siRNAs and 16 PEIs, while the number of native and modified PEIs is varied to achieve the desired substitution amounts. For example, in system α = 0.25, we placed 12 native PEIs and 4 PEI-1PrAs, and α is calculated based on the ratio of the number of modified PEIs to the total number of native and modified PEIs, that is, 4/(4 + 12) = 0.25. Similarly, in system α = 0.75, we placed 4 native PEIs and 12 PEI-1PrAs, and α is 12/(4 + 12) = 0.75. Composition and details of the studied systems are given in Table 1. In the initial configurations of the simulations systems (Figure 3, left and middle), the principal axes of all the molecules were aligned parallel to one another. Four siRNA molecules were then placed on the corners of a square with a side length of 13 Å. Center of mass (COM) of the PEIs, native and/or modified, was positioned 17 Å away from the COM of their neighboring siRNAs. In each system studied, four PEIs were placed amidst the 4 siRNAs, and the remaining 12 PEIs were placed symmetrically to surround the siRNAs. Systems were solvated in a rectangular TIP3P water box with a minimum margin of 15 Å from all the sides. Proper amount of K^+ and Cl^- ions were then added to achieve 150 mM physiological salt concentration to mimic intracellular environment.

Simulation Details. PEI topology was constructed by adopting the parameters of analogous molecules from CHARMM force field as outlined in CHARMM General Force Field methodology.[21] The validation for this approach of creating PEI topology was performed in our previous work.[17,22] For all the other molecules, CHARMM27 force field[23−26] was used. All the simulations were performed with MD package of NAMD[20] with a time step of 2 fs and periodic boundary conditions. Cut-off for van der Waals and pairwise electrostatic interactions was set to 12 Å, particle mesh Ewald[27] was used in the treatment of electrostatic interactions. Bonds involving hydrogen atoms were constrained with SHAKE algorithm.[28] All systems were first minimized for 5000 steps and then heated for 20 ps from 0 to 300 K, with a harmonic restraint (10 kcal/mol·Å^2) on solute's non-hydrogen atoms. Restraint on the non-hydrogen atoms of the solute was kept for another 10 ns. Restraint was then removed, and NPT simulations were performed for 200 ns. Langevin dynamics thermostat was used for temperature control, with thermostat damping coefficient of 10 ps^{-1} for all the non-hydrogen atoms. Pressure control was performed with Nosé−Hoover−Langevin barostat, with damping time scale of 100 fs and Langevin piston oscillation period of 200 fs. Visualization and analysis of the trajectories are performed with VMD.[19] For all the systems studied, dynamic equilibrium was observed to be achieved by 120 ns of the simulations. Therefore, unless otherwise specified, the data analysis will be based on the last 80 ns.

3. RESULTS

3.1. siRNA Delivery and Its Silencing Activity in K562 Cells. Delivery of FAM-labeled siRNA with native and PrA-modified PEIs was investigated in K562 cells. The cellular uptake and silencing data are presented in Figure 4. From flow cytometry analysis, substitution of PrA at low amounts, α = 0.26 and α = 0.69, resulted in substantially higher delivery than the native PEI (α = 0); FAM-siRNA delivery was 11- and 10-fold greater than α = 0 in α = 0.26 and 0.69 systems, respectively (based on the MFI of FAM-siRNA). Increasing the substitution amount α further to 1.14 and 1.59, however,

DOI: 10.1021/acsami.5b07929
ACS Appl. Mater. Interfaces 2015, 7, 24822−24832

Table 1. Details of the Five Simulated Systems

substitution amount (α)	PEIs simulated	siRNA/PEI charge ratio	number of atoms	number of K^+/Cl^-	size of the simulation box (Å^3)
0	16 native PEI	160/192	106 781	92/124	104 × 114 × 99
0.25	12 native PEI 4 PEI-1PrA	160/192	106 813	92/124	104 × 114 × 99
0.75	4 native PEI 12 PEI-1PrA	160/192	111 514	96/128	108 × 114 × 99
1	16 PEI-1PrA	160/192	108 324	93/125	107 × 112 × 99
2	16 PEI-2PrA	160/192	108 086	93/125	105 × 115 × 99

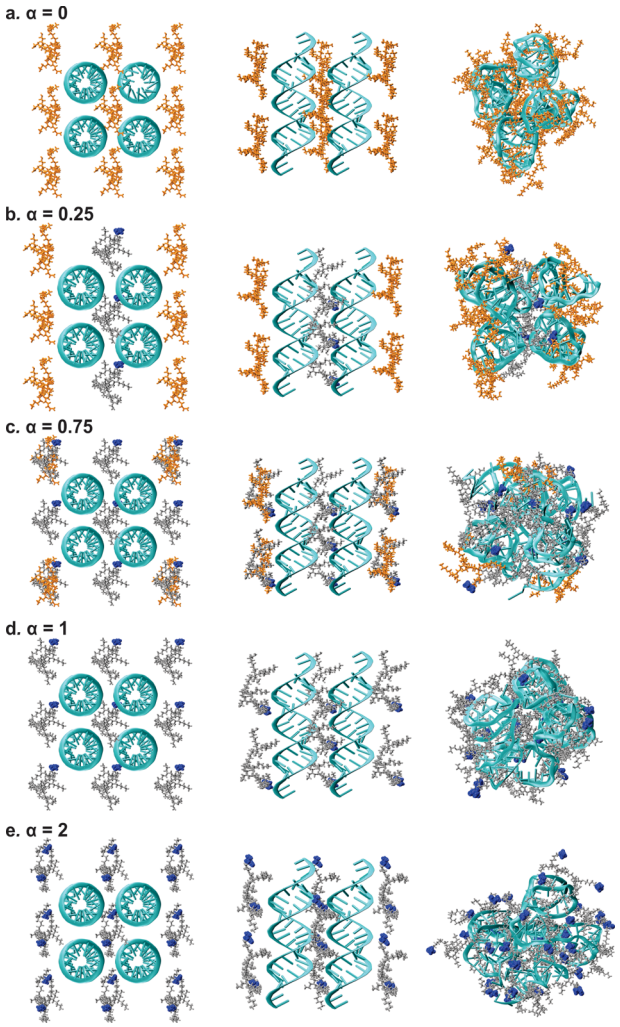

Figure 3. Initial ((left) top view and (middle) side view) and final ((right) top view) configurations of the simulated systems. (a) α = 0, (b) α = 0.25, (c) α = 0.75, (d) α = 1, (e) α = 2. siRNAs are given in cyan, native PEIs are in orange, and modified PEIs are in silver. PrA substitutions are represented as blue spheres. Water and ions are removed for clarity.

resulted in a significant decrease in the uptake efficiency of siRNA, where the mean delivery became almost comparable to that of native PEI (Figure 4a). Proportion of FAM-siRNA positive cells was well-correlated with the change in MFI. Delivery with native PEI resulted in 2.7 ± 0.8% FAM-siRNA positive population, while PEIs with α = 0.26 and α = 0.69 yielded 48.4 ± 2.5% and 44.1 ± 0.5% FAM-siRNA-positive cells, respectively. Further increase in the substitution amount decreased the positive population, where the smallest proportion (4.1 ± 1.4%) of siRNA-positive cells was obtained at the highest, α = 1.59 (Figure 4b). We also compared the performance of PrA-modified 1.2 kDa PEIs in delivering the siRNA with that of versatile carrier HMW (25 kDa) branched PEI. Low substitution ratios displayed a comparable performance to that of 25 kDa PEI, that is, in comparison to MFI of 25 kDa PEI, ∼twofold decrease in MFI was observed in systems α = 0.26 and α = 0.69 (Section S2 in Supporting Information, Figure S2a,b).

To explore the effect of PrA substitution on resulting silencing activity of delivered siRNA, we investigated GFP silencing in GFP-expressing K562 cells. GFP silencing was measured at 3, 6, and 9 d post transfection and represented with percent decrease in GFP MFI (normalized against no treatment; Figure 4c) and decrease in the proportion of GFP-positive cells (d). After 3 d, native PEI (α = 0) resulted in 5.2 ± 2.3% decrease in GFP MFI, while PEIs with α = 0.26 and α = 0.69 yielded 9.6 ± 1.5% and 32.9 ± 2.5% decreases, respectively. Substitution of more PrAs on PEI, however, decreased siRNA silencing activity; percent reduction in GFP MFI was 9.0 ± 1.9% and 4.3 ± 1.6% in polymers with α = 1.14 and α = 1.59, respectively (Figure 4c). The extent of silenced cell population was well-correlated with the percent decrease in GFP MFI, that is, 2.5 ± 0.4%, 5.4 ± 0.7%, 19.1 ± 2.2%, 3.5 ± 1.2%, and 1.9 ± 0.2% of the population was silenced with polymers α = 0, α = 0.26, α = 0.69, α = 1.14, and α = 1.59 systems, respectively, 3 d after the treatment (Figure 4d). The silencing activity of siRNA reached maximum at 6 d post transfection, after which a reduction in silencing efficiency was observed on day 9. For example, the decrease in GFP MFI was 32.9 ± 2.5%, 44.2 ± 3.3%, and 31.2 ± 1.0% for 3, 6, and 9 d with the polymer with α = 0.69 (best performing polymer). We also compared the efficacy of PrA-conjugated 1.2 kDa PEIs with 25 kDa PEI in terms of the silencing activity of the delivered siRNAs (Figure S2 in Section S2 of Supporting Information). Among others, PEI with α = 0.69 displayed a comparable albeit not superior performance to that of 25 kDa PEI (Figure S2c,d).

To further examine the effect of PrA substitution on the cellular interactions of polyplexes, we investigated the cytotoxicity of siRNA complexes prepared with polymers of different substitution amounts (Figure 5). Toxicity of the polyplexes increased with the increase in the polymer:siRNA weight ratio regardless of the PrA substitution amount (with α = 0 reaching plateau after polymer:siRNA ratio of 20:1), and >85% of the cells were viable at the polymer:siRNA weight ratio used in transfection studies (6:1). At the highest polymer:siRNA weight ratio tested, among different substitution amounts, α = 0.69 induced the highest toxicity followed by α = 0.26, with 28.4 ± 1.1% and 36.9 ± 3.6% cell viabilities, respectively. While α = 1.14 displayed intermediate toxicity levels with 52.3 ± 3.9% cell viability; toxicity is significantly reduced in α = 1.59 and was similar to that of the native PEI (α = 0), 77.9 ± 2.3% of cells were viable in α = 1.59 compared to 79.7 ± 8.6% in the unmodified system (Figure 5, inset). In line with the trends observed in the cellular uptake and silencing experiments, PrA substitution at low amounts (α = 0.26 and 0.69) resulted in increased cellular interactions (hence

DOI: 10.1021/acsami.5b07929
ACS Appl. Mater. Interfaces 2015, 7, 24822−24832

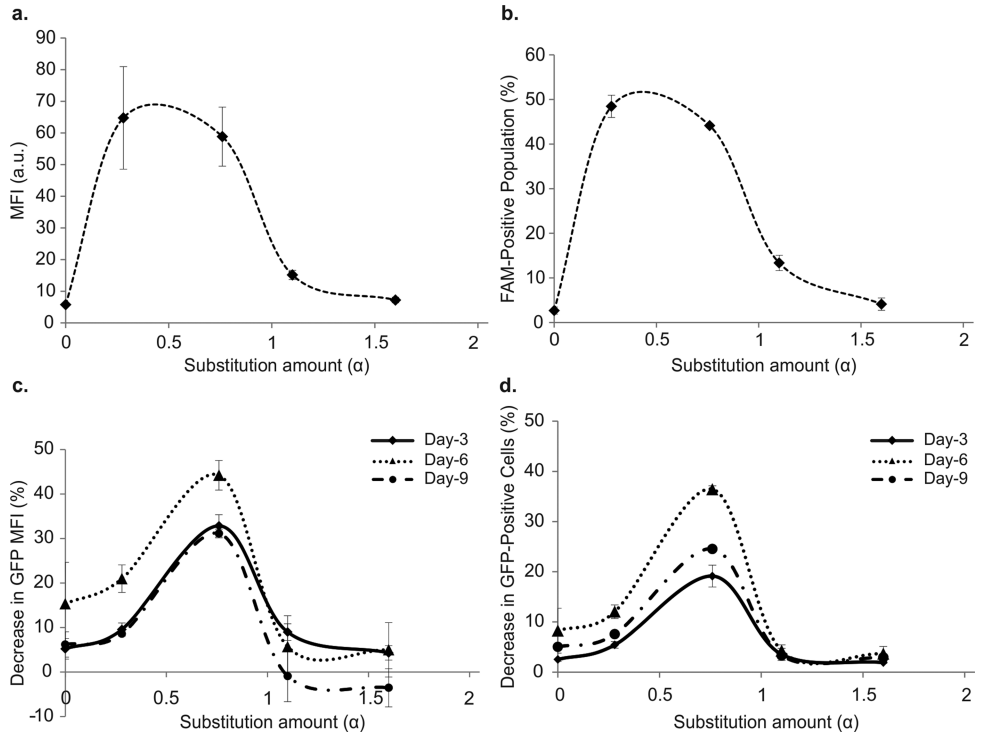

Figure 4. (a) Mean fluorescence intensity and (b) percentage of FAM-siRNA positive K562 cells after 24 h of exposure to polyplexes prepared with FAM-labeled siRNA and native or modified PEIs at polymer:siRNA ratio of 6:1 (w:w), with final siRNA concentration of 60 nM. (c) Decrease in mean GFP fluorescence and (d) decrease in GFP-positive cell population after 3, 6, and 9 d of treatment with final siRNA concentration of 60 nM at polymer:siRNA ratio of 6:1 (w:w).

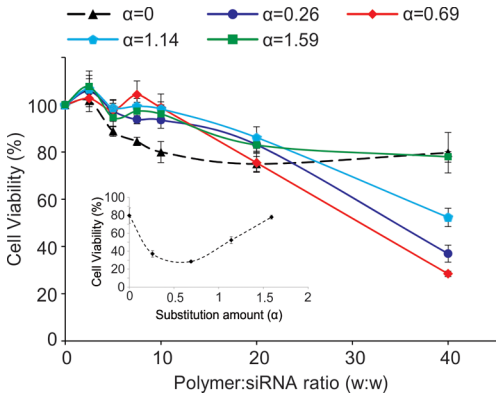

Figure 5. Relative viability of K562 cells after 72 h of exposure to polyplexes of different PrA substitution amounts prepared at various polymer:siRNA (w/w) ratios. (inset) The relative cell viability as a function of PrA substitution amount (α) at polymer:siRNA (w:w) ratio of 40:1.

cytotoxicity), while further increase in the substitution amount gradually reduced the toxicity of the polymers, with highest substitution reaching the toxicity of the native PEI. We also compared the cytotoxicity of native and PrA modified 1.2 kDa PEIs with 25 kDa PEI, and reported LMW native and/or modified PEIs to be substantially less toxic than their HMW counterpart at the highest polymer:siRNA weight ratios studied (Figure S3 in Section S2 of Supporting Information).

3.2. Mechanism for the Existence of Optimal Modification. From the experiments, it is clear that there is an optimal ratio for the modification of PEI with PrA groups, since grafting excess PrAs into PEI's structure abolished the siRNA delivery and its silencing activity in K562 cells. We therefore performed all-atom MD simulations to gain a better understanding of the change in PEI's performance by monitoring the molecular-level interactions governing the complexation of siRNAs with hydrophobically modified PEIs. Final configurations of the simulation systems are given in right panel of Figure 3. The abilities of native and modified PEIs to complex and compact the siRNAs were assessed by calculating the radii of gyration (R_g) of four siRNAs in each system (Figure 6a). The decreasing R_g observed in the first 120 ns of the simulations is an indicator of the complexation process of siRNAs with the PEIs. Differences were observed in the kinetics of complexation among different simulation systems, that is, in the system $\alpha = 0.75$, R_g of the four siRNAs is lower than that of others between ~38 and 73 ns, while $\alpha = 1$ gives higher R_g values among all systems within the first 30 ns and between 70−100 ns. Despite the differences observed in complexation kinetics, all the simulation systems reached plateau over the last 80 ns of the simulations. The average R_g values were calculated to be 25.86 ± 0.19, 25.71 ± 0.17, 25.94 ± 0.17, 25.85 ± 0.14, and 26.00 ± 0.16 Å for the systems $\alpha = 0$, $\alpha = 0.25$, $\alpha = 0.75$, $\alpha = 1$, and $\alpha = 2$, respectively (Figure 6b). Given the similar values of R_g observed in each system, substitution of PrA did not seem to affect PEI's ability to compact siRNAs. We also explored the influence of PrA substitution on the compactness of the polyplexes by including all the siRNA and PEIs in the calculation of R_g and again observed the almost negligible effect of modification (Figure S4 of Supporting Information). The sizes of the particles, prepared at polymer:siRNA weight ratio of 6:1, were experimentally measured; the PrA substitution on the polymers did not show a clear trend on the hydrodynamic size of polyplexes, with particles ranging between 150 and 400 nm (Figure S5 of Supporting Information).

DOI: 10.1021/acsami.5b07929
ACS Appl. Mater. Interfaces 2015, 7, 24822−24832

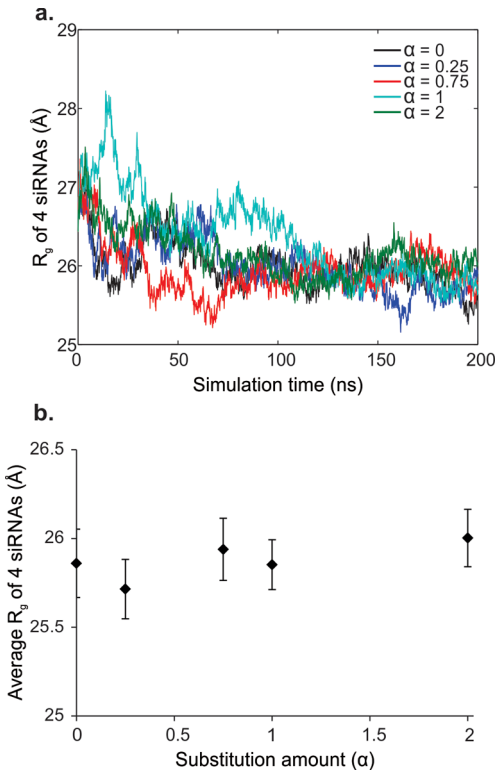

Figure 6. (a) R_g of the four siRNAs as a function of simulation time and (b) average R_g values of the four siRNAs calculated over the last 80 ns of the simulations as a function of substitution amount (α).

The motion and the location of the hydrophobic moieties during polyplex formation are expected to be critical in determining the performance of polyplexes. In order to monitor the location of PrA moieties, we calculated the radial distribution function (RDF) of PrA carbon atoms as a function of the distance r (in Å) from the COM of polyplex (Figure 7).

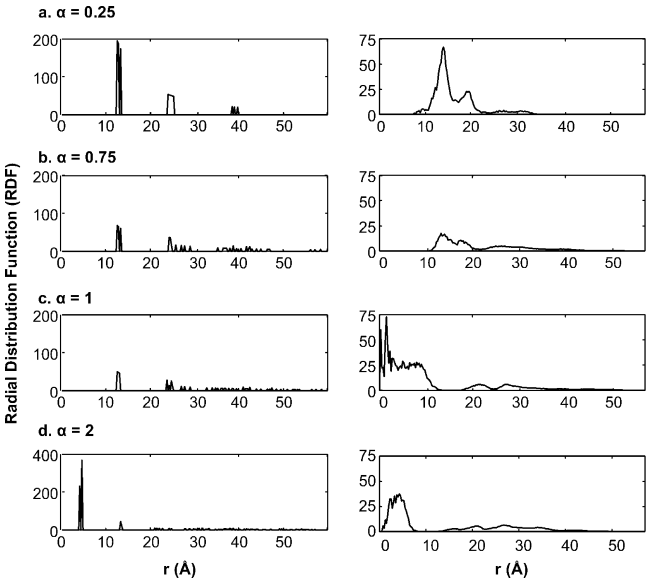

Figure 7. RDF of carbon atoms of hydrophobic PrA moieties, in the initial configuration (left), and the average over the last 80 ns of the simulations (right), in the systems (a) α = 0.25, (b) α = 0.75, (c) α = 1, and (d) α = 2, respectively.

Initial distribution of PrA carbons (Figure 7, left) is similar for systems α = 0.25, α = 0.75, and α = 1 due to the similar arrangement of molecules in the initial configurations. The decrease in peak heights as α increases indicates the distribution of PrA becomes more homogeneous with the increase in the substitution amount. In the system α = 2, the most pronounced peak appears at smaller r because of the much more PrA carbon atoms it involves, which resulted in denser distribution of PrA close to the COM of the polyplex. As the systems reach dynamic equilibrium (Figure 7, right), in the system α = 0.25, the first and most prominent peak is observed at r = 13.88 Å, followed by the second peak located at r = 18.88 Å. Similarly, in the system α = 0.75, two peaks are present, the first located at r = 13.38 Å and the second at r = 17.63 Å. Between these two low-substituted systems, a more uniform distribution is observed as the extent of PrA substitution increased from 0.25 to 0.75. No significant changes are apparent in the motion of PrA substituents between initial and final configurations; in particular, there are no PrA moieties within the 10 Å from the COM of the polyplexes. The most drastic change is observed in the system α = 1; the hydrophobic moieties started to migrate into the core region of the polyplex, indicated by the two sharp peaks located as close to the COM of the polyplex as 0.38 and 1.63 Å. Clearly, a considerable number of PrA moieties are now distributed within the first 10 Å from the COM of the polyplex, as opposed to being located beyond 10 Å as observed in the α = 0.25 and α = 0.75 systems. This phenomenon holds true in the system α = 2 as well; however, it should be considered that some PrA carbon atoms were already present within 5 Å of the COM of the polyplex in its initial configuration.

Since surface hydrophobicity might influence complex interactions with cell membranes (and uptake), the migration of PrA moieties into the core of the polyplex at high substitution ratios raises the question of the density of PrA groups on particle surfaces. To assess the surface PrA density, we approximated each polyplex by a sphere and determined the radius of the sphere by using the R_g of the polyplex. The number of PrA Cs outside the spherical surface is then counted from the number integral over RDF of PrA Cs averaged over the last 80 ns of the simulations (Figure S6 of the Supporting Information) and divided by the surface area of the sphere (details on the calculation is given in Section S4 of Supporting Information). The calculated surface density is plotted in Figure 8a. A nonmonotonic change in the surface PrA density is observed with the increase in the extent of substitution. Lower substitution ratios resulted in lower surface densities. As a consequence of having all the modified PEIs amidst the four siRNAs, there are no PrA moieties on the surface in the system α = 0.25. In the system α = 0.75, however, all the modified PEIs were placed homogeneously to surround the four siRNAs; hence, there is a slight increase in the surface density of PrAs. Apart from the differences in the number of PrA moieties, the initial configurations of the systems α = 1 and α = 2 are similar to that of α = 0.75. The highest surface density is observed in system α = 1 among all systems; however, further increasing the substitution extent to α = 2 lowered the surface groups. This could be explained in the context of hydrophobic interactions that minimize the number of PrA moieties exposed to water via the migration to the core (Figure 7c,d), as observed above. However, if the hydrophobic interactions are not strong enough to drive the PrAs to the core, a considerable number of PrAs still remains on the surface, as in the case of the system α = 1. Increasing the substitution extent to a higher level (α = 2)

DOI: 10.1021/acsami.5b07929
ACS Appl. Mater. Interfaces 2015, 7, 24822−24832

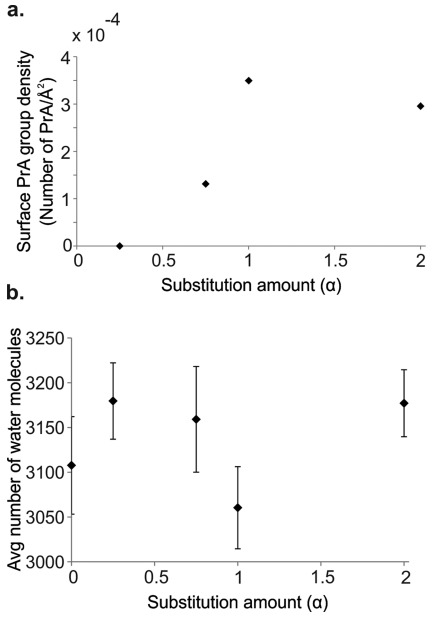

Figure 8. (a) Surface density of the PrA moieties and (b) number of water molecules in the hydration shell of siRNAs/PEIs, as a function of the substitution amount (α).

provided enough hydrophobic driving force and, hence, lowered the surface density. The proportions of the PrA moieties inside the polyplexes are in fact 100%, 91%, 82%, and 92% for the systems α = 0.25, α = 0.75, α = 1, and α = 2, respectively. Considering the number of PrA Cs in the system α = 2 (= 96), it is evident that it has the most hydrophobic core among all systems.

The variation in the surface density of the PrA moieties made us wonder about the change in the surface hydration of polyplexes. Hydration of the surfaces with hydrophobic domains plays a major role in biomolecular recognition;[29,30] hence, to explore the level of hydration of polyplexes in a quantitative manner, we calculated the number of water molecules in the hydration shell of siRNAs and PEIs. Here we define the hydration shell to be 3 Å from any siRNA/PEI atom. As the polyplexes are formed, water molecules are expelled from their interior locations to the periphery (Section S5 in Supporting Information). The average number of water molecules in the hydration shell upon reaching dynamic equilibrium is plotted in Figure 8b. An inverse correlation can be observed between the surface density of PrA groups (Figure 8a) and the level of hydration. As a consequence of the lower PrA surface density of the systems α = 0.25, α = 0.75, and α = 2, the polyplexes are more hydrated given by the higher number of water molecules in the hydration shell. Loss of hydration in the system α = 1 is due to water molecules being expelled from the periphery as a result of the high PrA surface density, revealing the polyplex formed at α = 1 to be the most hydrophobic one among others.

To explore the effect of substituted PrA moieties on PEI's binding capability to siRNA, we plot the number of PEI Ns in close contact with siRNA N/O atoms (Figure 9a). Here we define the close contact distance to be 4 Å from any siRNA N/Os, that is, the distance at which a direct H-bond could be formed between PEI amines and siRNA N/O atoms.[17] Grafting PrAs into PEIs structure increased the interactions between PEIs and siRNAs in general, given the upward trend in the

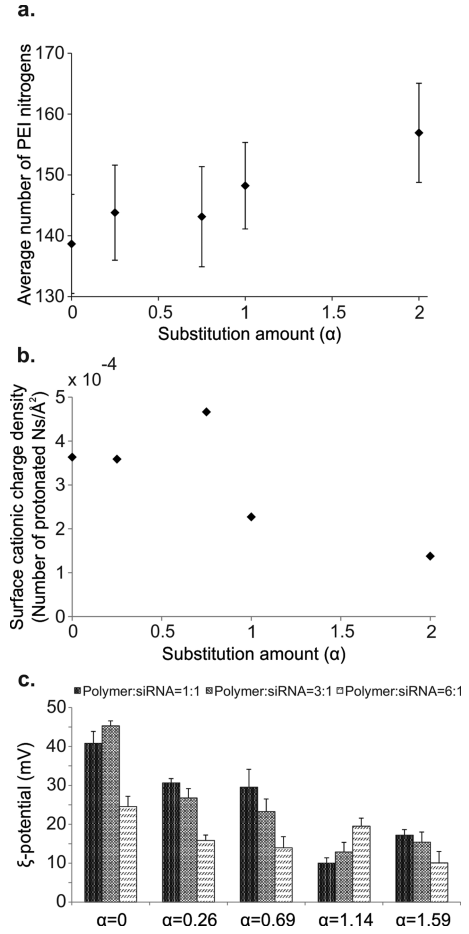

Figure 9. (a) Average number of PEI nitrogen atoms in close contact with siRNAs and (b) surface cationic charge density, as a function of the substitution amount (α). (c) ζ-potential of the polyplexes of different substitution amounts, prepared at polymer:siRNA weight ratios of 1:1, 3:1, and 6:1.

number of close contacts established with the increase in the substitution extent, with α = 2 giving the highest number. The hydrophobic attractions among PrA moieties drive them to the core of the polyplex, along with their associated PEIs. Clustering in the core area, then, increases the number of PEI Ns in close contact with siRNAs, evident from the higher number of close contacts established in systems α = 1 and α = 2 in comparison with the lower-substituted systems.

The higher number of contacts established between siRNAs and PEIs in high substitution amounts due to PrA migration into the core could possibly affect the assembly of cationic amine groups on the polyplex surfaces and, hence, might have an impact on their cellular uptake. To monitor the change in the cationic surface charge of polyplexes with PrA substitution amounts, we explored the density of protonated PEI Ns on the surface of the polyplexes by following the procedure described previously for the definition of the spherical polyplex surfaces. The number of protonated PEI Ns outside the spherical surface is then counted from the number integral over the RDF of protonated PEI Ns averaged over the last 80 ns of the simulations (Figure S9b of Supporting Information) and divided by the surface area of the sphere (details are given in Section S6 of Supporting Information). The resulting surface cationic charge density is plotted in Figure 9b. Moderate enhancements in the hydrophobicity of the polyplexes gave rise

DOI: 10.1021/acsami.5b07929
ACS Appl. Mater. Interfaces 2015, 7, 24822−24832

to a higher cationic surface charge in comparison with the unmodified system ($\alpha = 0$); $\alpha = 0.75$ had the highest cationic surface charge among all systems. However, further increasing the substitution extent significantly reduced the number of cationic groups on the surface. In fact, systems $\alpha = 1$ and $\alpha = 2$ have substantially lower cationic surface charge than the unmodified system, $\alpha = 0$, with $\alpha = 2$ giving the lowest surface charge. It is evident that the new assembly mechanism brought about by the high amount of PrA moieties affected the complexation between siRNAs and PEIs and caused the PEIs to be dragged to the core, which in turn resulted in a deleterious effect on the cationic surface charge of the polyplexes. Surface charge (ζ-potential) of the particles was also investigated to explore the effect of PrA substitution experimentally (Figure 9c). Polyplexes were prepared at different polymer:siRNA ratios (1:1, 3:1, and 6:1). We observed slightly more positively charged particles (higher ζ-potential) for $\alpha = 0$, 0.26, and 0.69 in polymer:siRNA weight ratios of 1:1 and 3:1 than the highest ratio tested, 6:1. A decreasing trend in ζ-potential with the increase in PrA substitution amount was apparent irrespective of the polymer:siRNA weight ratio studied; however, it was more pronounced at the lower polymer:siRNA weight ratios, 1:1 and 3:1. Along the lines of the surface charge of polyplexes from the simulation trajectories, here we report the adverse effect of excess PrA substitution on the surface charge of the polyplexes again, with more than twofold decrease from $\alpha = 0$ to $\alpha = 1.59$ in all the polymer:siRNA weight ratios tested.

Nonbonded interactions with PEIs might cause changes in siRNA structure. Hydrogen bonding is critical in maintaining the structure of nucleic acids via Watson−Crick base pairing; therefore, we examined the hydrogen bonding pattern between the two strands of siRNAs during polyplex formation. The downward trend within the first ∼100 ns of the simulations indicates the loss of siRNAs' structure as a result of complexation (Figure S10a of Supporting Information). For a quantitative analysis of structural changes, the total number of hydrogen bonds is averaged upon reaching dynamic equilibrium (Figure 10a). In comparison with the unmodified system ($\alpha = 0$), PrA substitution altered the structure of siRNAs given by the loss of hydrogen bonding in systems $\alpha = 0.25$, $\alpha = 0.75$, and $\alpha = 2$. Considering the majority of the PrA moieties are located inside of the polyplexes at these substitution ratios, alterations in siRNA's structure are expected as a result of the steric effect introduced by PrA moieties. Consistent with its highest surface PrA density, the most stable siRNA structure is achieved in the system $\alpha = 1$.

The structural changes in siRNA upon complexation can be further confirmed by examining the root-mean-square deviation (RMSD) of the four siRNAs with respect to their initial configuration (Figure 10b). The time evolutions of the RMSD for the four systems are given in Figure S10b in Section S7 of Supporting Information. The upward trend within the first ∼120 ns is due to the profound deviations caused by polyplex formation. The systems $\alpha = 0$, $\alpha = 0.25$, and $\alpha = 1$ displayed very similar RMSD trends throughout the simulations. The relatively higher deviation in the system $\alpha = 0.75$ could be attributed to its kinetics of complexation, that is, two PrA-substituted PEIs were observed to be fully solvated within the first ∼110 ns, and they established contacts with the polyplex at ∼110 and ∼140 ns, respectively, causing siRNAs to be more deviated as a result of having more polymers in contact. Among all the other systems, the highest deviation is observed with the system $\alpha = 2$. Supporting the previous discussion on the migration of PrA moieties to the polyplex core, having more contacts built with PEIs and losing siRNA structure at the highest substitution, the highest deviation is observed at $\alpha = 2$.

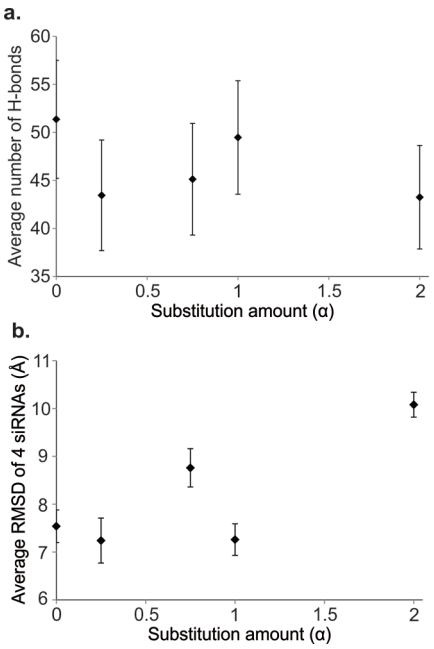

Figure 10. (a) Total number of siRNA hydrogen bonds. Each system has four siRNA molecules; the hydrogen bonds established between the two strands of each siRNA is summed over the four siRNA molecules and then averaged over the last 80 ns. (b) RMSD values of the four siRNAs with respect to their initial configurations as a function of the substitution amount (α).

3.3. Discussion. PrA modifications investigated in this work were aimed to increase the performance of less cytotoxic albeit nonfunctional LMW PEI. Enhancements in PEI's gene delivery capability and resulting gene silencing capacity of siRNA were observed at low substitution amounts; whereas a significant reduction in PEI's performance was detected as the extent of PrA substitution, hence, the hydrophobicity of PEI increased further. This interesting observation suggests that a certain balance between hydrophobicity and hydrophilicity is needed to achieve the optimal transfection efficiency and silencing capability. This was not the case with moderately longer-chain aliphatic lipid substituents (8C substitution), where a gradual increase in transfection efficiency was obtained in proportion with substitution amounts. However, a similar phenomenon was reported previously by others with shorter hydrophobes. Conjugation of varying lengths of alkyl chains, ethyl, octyl, and deodecyl, into 1.8 kDa PEI showed that shorter hydrophobic substituent ethyl was capable of inducing higher transfection efficiencies than their longer counterparts octyl and deodecyl. Moreover, extending the conjugation degree of ethyl resulted in higher transfection at the intermediate conjugation levels, while at the highest substitution (i.e., when 100% of the amines were conjugated) transfection efficiency of PEI was drastically decreased.[14] A different study explored the effect of hydrophobic/hydrophilic balance of 25 kDa PEI on its performance by grafting amino acids, one with a short side chain, alanine (Ala, 1C), and one with a longer side chain, leucine (Leu, 4C). They reported that moderate enhancements on the hydrophobicity of 25 kDa PEI via conjugation of Ala resulted in higher transfection efficiencies than the engraftment of Leu.[31] Although these experimental studies revealed the importance of

DOI: 10.1021/acsami.5b07929
ACS Appl. Mater. Interfaces 2015, 7, 24822−24832

hydrophobic/hydrophilic balance of carrier vectors for an optimal performance, no mechanistic findings were reported to explain the deleterious effects of increasing hydrophobicity. It was proposed that hydrophobic groups cluster together and possibly affect PEI's protonation ratio,[31] but no evidence was provided to validate this hypothesis.

Experiments accompanied by MD simulations on caprylic (8C) and linoleic acid (18C) substituted 2 kDa PEI revealed one possible mechanism for nonmonotonic relationship between substitution level and cellular uptake. Increasing the substitution extent of caprylic acid was reported to improve siRNA delivery monotonically from in vitro experiments. In line with experimental observations, MD simulations indicated higher polyplex stability in the presence of more caprylic acid substituents, due to the stabilizing effect of enhanced lipid−lipid association among different PEI molecules. Increasing the substitution extent of linoleic acid, however, did not always lead to an increase in PEI's performance. MD trajectories showed self-association of the aliphatic lipid tails located on the same PEI molecule, which gave rise to steric hindrance and adversely influenced siRNA complexation.[17] In this work, due to PrA's short nature, association of PrA groups was not observed. However, gradual increase in the extent of PrA substitution gave rise to an interesting phenomenon, namely, migration of hydrophobic PrA groups into the polyplex core to minimize the interactions with the aqueous phase. Clustering in the polyplex core in the highest substitution caused a reduction in the surface density of PrA groups and hence the surface hydrophobicity. Peripheral hydrophobic moieties may facilitate the complex interactions with plasma membrane and expedite the cellular uptake of polyplexes. Absence of surface hydrophobicity might possibly impede and/or abolish the uptake, especially if the surface cationic charge is not sufficient to protect and translocate the siRNA cargo along the delivery path. We reported that, although all the simulated native and modified PEIs carried the same cationic charge, intermediate PrA substitution amounts gave rise to a higher cationic charge on the polyplex surface compared to the unmodified and low-substituted systems, whereas surface cationic charge of the polyplexes was drastically decreased as the extent of substitution was increased. The hydrophobic force driving the PrA moieties into the core dragged the associated PEIs; that was evident from the highest number of PEI Ns in close contact with siRNAs at the highest amount of PrA substitution. This, in turn, reduced the amount of PEI's protonated amine groups on the polyplex surface. A relationship with the cationic surface charge and the assembly mechanism of carrier vectors was previously reported by Posocco and co-workers.[32] The analysis performed from the mesoscale simulation trajectories revealed that different self-assembly mechanisms brought by cholesterol-modified generations 1 and 2 spermine dendrimers controlled the cationic surface charge density of the aggregates. Less effective dendrimer assembly led to a reduction in cationic surface charge, which affected their DNA packing capability as a consequence.[32] In line with their argument, here we reported that the new complexation mechanism induced by the presence of the abundant PrA moieties has a profound effect on the cationic surface charge of the polyplexes. This phenomenon was further validated with experimental ζ-potential measurements, where we reported more than twofold decrease in the surface charge at the highest PrA substitution amount in comparison with the unmodified polymer. Moreover, cationic surface charge of the nanoparticles has known to possibly induce membrane damage and hence cytotoxicity.[33] MTT assay showed polymers with low/moderate PrA substitution amounts to be more toxic than their highly substituted counterparts at high polymer concentrations. This is, again, another indication of the loss of the cationic charge in the presence of abundant PrA modifications. Coupled with the loss of surface hydrophobicity at the highest substitution, it resulted in loss of cellular uptake and gene silencing capability of siRNA, as is evident from the in vitro experiments.

The structural stability of siRNA is also affected by clustering of PrA moieties at the core of the polyplex. Both the hydrogen bonding and RMSD data provided such evidence; that is, at the highest substitution amount, siRNAs deviated the most with respect to their initial configurations while displaying a reduced amount of hydrogen bonding compared to that of unmodified PEI. Loss of siRNA's structural stability is worrisome as it could most likely affect the overall activity of the siRNA and hence the desired pharmaceutical effect. Coupling the changes in the surface hydrophobicity and cationic charge density of the polyplexes with the observed structural instabilities, siRNAs might become more vulnerable to degrading nucleases in the presence of abundant PrA modifications on PEIs, which consequently might cause the loss of siRNA's biological activity.

3.4. Limitations. MD simulations provide invaluable information at the molecular level; however, current computing resources available limit the size and time scale that can be simulated to a few nanometers and microseconds range. Despite the discrepancy in the length and time scale between real life experiments and computer simulations, computational tools have been used to study the dynamics of biosystems since the very first protein (bovine pancreatic trypsin inhibitor) simulation performed in 1977,[34] and they have been successfully used for complex biological systems over the last three decades. Although simulation trajectories cannot provide macroscopic details at times, the atomistic data acquired at the nanoscale could be used to predict the macroscopic properties. The sizes of our simulated polyplexes are ∼4 nm, while we report the real sizes of the corresponding particles to be 150−400 nm. While direct correlations should not be sought between experiments and simulations on this aspect, our computational data are in good agreement with observed trends in experiments; that is, the insignificant effect of PrA modification on the size of the polyplexes and the deleterious effect of excess PrA modification on the cationic surface charge of polyplexes were observed. Moreover, the simulations provide a mechanistic explanation to the experimental observations, which is not possible to obtain with current experimental tools at our disposal.

Time scale is another limitation of the MD techniques. One must perform simulations long enough to observe dynamic equilibrium and obtain accurate results. The risk of the simulated systems being trapped in a potential energy well does always exist; therefore, the resulting configuration could be one of the possible configurations, albeit not the most probable. Enhanced sampling techniques, such as umbrella sampling and replica exchange MD, have been developed to overcome this barrier and could be used to improve the accuracy of the results. Our simulations on polyplex formation from siRNA and PrA-modified PEIs were performed for 200 ns, whereas polyplex formation takes place on the scale of minutes in real life. Despite its short time frame, our simulations are in fact longer than the majority of the published all-atom simulations in the field, which were on the order of 10−20

DOI: 10.1021/acsami.5b07929
ACS Appl. Mater. Interfaces 2015, 7, 24822−24832

ns for binding of polycationic carriers to nucleic acids.[35−37] We also note that we studied our simulation trajectories for the existence of dynamic equilibrium in many ways (i.e., observation of plateau in R_g of the particles and H-bonds between siRNAs, to name a few), and interpreted our data only over the equilibrium period, last 80 ns of the simulations. Although techniques, such as coarse graining (CG), were developed to overcome time restrictions, their major drawback is the loss of atomistic information and, hence, the accuracy for chemical translation. Therefore, we performed our simulations in the atomistic scale to fully understand the mechanism brought by the presence of PrA moieties.

4. CONCLUSIONS

LMW (1.2 kDa) PEI was hydrophobically modified with varying amounts of PrA moieties. Cellular uptake and silencing activity of the polyplexes was enhanced at low/moderate substitution amounts, while further increase in PrA substitution abolished siRNA uptake and hence the silencing activity. All-atom MD simulations revealed a new siRNA-PEI assembly mechanism in the presence of abundant PrA substituents: PrA moieties were observed to migrate into the core region of the polyplex under the hydrophobic driving force for minimizing their exposure to the aqueous phase. This new assembly mechanism led to (i) higher surface hydrophobicity and (ii) higher surface charge density at intermediate substitution amount, while increasing the substitution extent further caused detrimental changes on surface hydrophobicity and cationic charge density, as well as siRNA stability. The molecular details obtained from the simulation trajectories elucidated possible mechanistic details on the effect of hydrophobic/hydrophilic balance of the carrier vectors in polyplex assembly and the resulting structure−function relationships, and they should provide valuable insights in the design of novel hydrophobic substituents.

■ ASSOCIATED CONTENT

Supporting Information

The Supporting Information is available free of charge on the ACS Publications website at DOI: 10.1021/acsami.5b07929.

Polymer synthesis and characterization, comparison of the efficacy and cytotoxicity of the PrA-modified PEIs with 25 kDa PEI, molecular details regarding the compactness of the polyplexes, experimental measurements of particle sizes, details on the calculation of PrA surface density, MD analyses on the location of water molecules, hydration of polyplexes, binding dynamics of PEI to siRNA and the stability of siRNAs during simulations. (PDF)

■ AUTHOR INFORMATION

Corresponding Authors

*E-mail: hasan.uludag@ualberta.ca. (H.U.)
*E-mail: tian.tang@ualberta.ca. (T.T.)

Notes

The authors declare no competing financial interest.

■ ACKNOWLEDGMENTS

Compute Canada and high-performance computing facility at National Institute for Nanotechnology, Edmonton, Canada, were gratefully acknowledged for providing computing resources and technical support. This work is funded by Natural Sciences and Engineering Research Council of Canada (T.T. and H.U.), Canadian Institutes of Health Research (H.U.), an NSERC CREATE Scholarship (H.U.; NCPRM from Univ. of Laval), Alberta Innovates-Technology Futures (T.T.), and Canada Foundation for Innovation (T.T.). We thank Dr. A. Lavasanifar (Faculty of Pharmacy & Pharmaceutical Sciences, Univ. of Alberta) for access to the Zetasizer.

■ REFERENCES

(1) Liu, Z.; Zhang, Z.; Zhou, C.; Jiao, Y. Hydrophobic Modifications of Cationic Polymers for Gene Delivery. *Prog. Polym. Sci.* **2010**, *35*, 1144−1162.

(2) Fire, A.; Xu, S.; Montgomery, M. K.; Kostas, S. A.; Driver, S. E.; Mello, C. C. Potent and Specific Genetic Interference by Double-stranded RNA in Caenorhabditis Elegans. *Nature* **1998**, *391*, 806−811.

(3) Boussif, O.; Lezoualc'h, F.; Zanta, M. A.; Mergny, M. D.; Scherman, D.; Demeneix, B.; Behr, J. P. A Versatile Vector for Gene and Oligonucleotide Transfer into Cells in Culture and In Vivo: Polyethylenimine. *Proc. Natl. Acad. Sci. U. S. A.* **1995**, *92*, 7297−7301.

(4) Demeneix, B.; Behr, J. P. Polyethylenimine (PEI). *Adv. Genet.* **2005**, *53*, 215−230.

(5) Aliabadi, H. M.; Landry, B.; Sun, C.; Tang, T.; Uludag, H. Supramolecular Assemblies in Functional siRNA Delivery: Where Do We Stand? *Biomaterials* **2012**, *33*, 2546−2569.

(6) Godbey, W. T.; Wu, K. K.; Mikos, A. G. Size Matters: Molecular Weight Affects the Efficiency of Poly(ethylenimine) as a Gene Delivery Vehicle. *J. Biomed. Mater. Res.* **1999**, *45*, 268−275.

(7) Fischer, D.; Bieber, T.; Li, Y.; Elsasser, H. P.; Kissel, T. A Novel Non-Viral Vector for DNA Delivery Based on Low Molecular Weight, Branched Polyethylenimine: Effect of Molecular Weight on Transfection Efficiency and Cytotoxicity. *Pharm. Res.* **1999**, *16*, 1273−1279.

(8) Fischer, D.; Li, Y.; Ahlemeyer, B.; Krieglstein, J.; Kissel, T. In Vitro Cytotoxicity Testing of Polycations: Influence of Polymer Structure on Cell Viability and Hemolysis. *Biomaterials* **2003**, *24*, 1121−1131.

(9) Neamnark, A.; Suwantong, O.; KC, R. B.; Hsu, C. Y.; Supaphol, P.; Uludag, H. Aliphatic Lipid Substitution on 2 kDa Polyethylenimine Improves Plasmid Delivery and Transgene Expression. *Mol. Pharmaceutics* **2009**, *6*, 1798−1815.

(10) Incani, V.; Lavasanifar, A.; Uludag, H. Lipid and Hydrophobic Modification of Cationic Carriers on Route to Superior Gene Vectors. *Soft Matter* **2010**, *6*, 2124−2138.

(11) Han, S.; Mahato, R. I.; Kim, S. W. Water-Soluble Lipopolymer for Gene Delivery. *Bioconjugate Chem.* **2001**, *12*, 337−345.

(12) Furgeson, D. Y.; Cohen, R. N.; Mahato, R. I.; Kim, S. W. Novel Water Insoluble Lipoparticulates for Gene Delivery. *Pharm. Res.* **2002**, *19*, 382−390.

(13) Bajaj, A.; Kondaiah, P.; Bhattacharya, S. Synthesis and Gene Transfection Efficacies of PEI-Cholesterol-based Lipopolymers. *Bioconjugate Chem.* **2008**, *19*, 1640−1651.

(14) Teo, P. Y.; Yang, C.; Hedrick, J. L.; Engler, A. C.; Coady, D. J.; Ghaem-Maghami, S.; George, A. J.; Yang, Y. Y. Hydrophobic Modification of Low Molecular Weight Polyethylenimine for Improved Gene Transfection. *Biomaterials* **2013**, *34*, 7971−7979.

(15) Pettersen, E. F.; Goddard, T. D.; Huang, C. C.; Couch, G. S.; Greenblatt, D. M.; Meng, E. C.; Ferrin, T. E. UCSF Chimera - A Visualization System for Exploratory Research and Analysis. *J. Comput. Chem.* **2004**, *25*, 1605−1612.

(16) Utsuno, K.; Uludag, H. Thermodynamics of Polyethlyenimine-DNA Binding and DNA Condensation. *Biophys. J.* **2010**, *99*, 201−207.

(17) Sun, C.; Tang, T.; Uludag, H. A Molecular Dynamics Simulation Study on the Effect of Lipid Substitution on Polyethylenimine Mediated siRNA Complexation. *Biomaterials* **2013**, *34*, 2822−2833.

(18) *Schrödinger Release 2014−2: Maestro, version 9.8;* Schrödinger, LLC: New York, NY, 2014.

(19) Humphrey, W.; Dalke, A.; Schulten, K. VMD: Visual Molecular Dynamics. *J. Mol. Graphics* **1996**, *14*, 33−38.

DOI: 10.1021/acsami.5b07929
ACS Appl. Mater. Interfaces 2015, 7, 24822−24832

(20) Phillips, J. C.; Braun, R.; Wang, W.; Gumbart, J.; Tajkhorshid, E.; Villa, E.; Chipot, C.; Skeel, R. D.; Kale, L.; Schulten, K. Scalable Molecular Dynamics with NAMD. *J. Comput. Chem.* **2005**, *26*, 1781−1802.
(21) Vanommeslaeghe, K.; Hatcher, E.; Acharya, C.; Kundu, S.; Zhong, S.; Shim, J.; Darian, E.; Guvench, O.; Lopes, P.; Vorobyov, I.; Mackerell, A. D., Jr. CHARMM General Force Field: A Force Field for Drug-like Molecules Compatible with the CHARMM All-atom Additive Biological Force Fields. *J. Comput. Chem.* **2010**, *31*, 671−690.
(22) Sun, C.; Tang, T.; Uludag, H.; Cuervo, J. E. Molecular Dynamics Simulations of DNA/PEI Complexes: Effect of PEI Branching and Protonation State. *Biophys. J.* **2011**, *100*, 2754−2763.
(23) Brooks, B. R.; Bruccoleri, R. E.; Olafson, B. D.; States, D. J.; Swaminathan, S.; Karplus, M. Charmm − A Program for Macromolecular Energy, Minimization, and Dynamics Calculations. *J. Comput. Chem.* **1983**, *4*, 187−217.
(24) MacKerell, A. D.; Brooks, B.; Brooks, C. L.; Nilsson, L.; Roux, B.; Won, Y.; Karplus, M. CHARMM: The Energy Function and Its Parameterization with an Overview of the Program. In *The Encyclopedia of Computational Chemistry;* John Wiley & Sons: Chichester, U.K., 1998; pp 271−277.
(25) Foloppe, N.; MacKerell, A. D., Jr. All-Atom Empirical Force Field for Nucleic Acids: I. Parameter Optimization Based on Small Molecule and Condensed Phase Macromolecular Target Data. *J. Comput. Chem.* **2000**, *21*, 86−104.
(26) MacKerell, A. D.; Banavali, N. K. All-atom Empirical Force Field for Nucleic Acids: II. Application to Molecular Dynamics Simulations of DNA and RNA in Solution. *J. Comput. Chem.* **2000**, *21*, 105−120.
(27) Darden, T.; York, D.; Pedersen, L. Particle Mesh Ewald: An N·log(N) Method for Ewald Sums in Large Systems. *J. Chem. Phys.* **1993**, *98*, 10089−10092.
(28) Ryckaert, J. P.; Ciccotti, G.; Berendsen, H. J. C. Numerical Integration of the Cartesian Equations of Motion of a System with Constraints: Molecular Dynamics of N-alkanes. *J. Comput. Phys.* **1977**, *23*, 327−341.
(29) Blokzijl, W.; Engberts, J. B. F. N. Hydrophobic Effects. Opinion and Facts. *Angew. Chem., Int. Ed. Engl.* **1993**, *32*, 1545−1579.
(30) Rossky, P. J.; Cheng, Y.-K. Surface Topography Dependence of Biomolecular Hydrophobic Hydration. *Nature* **1998**, *392*, 696−699.
(31) Thomas, M.; Klibanov, A. M. Enhancing Polyethylenimine's Delivery of Plasmid DNA into Mammalian Cells. *Proc. Natl. Acad. Sci. U. S. A.* **2002**, *99*, 14640−14645.
(32) Posocco, P.; Pricl, S.; Jones, S.; Barnard, A.; Smith, D. K. Less Is More − Multiscale Modelling of Self-assembling Multivalency and Its Impact on DNA Binding and Gene Delivery. *Chem. Sci.* **2010**, *1*, 393−404.
(33) Frohlich, E. The Role of Surface Charge in Cellular Uptake and Cytotoxicity of Medical Nanoparticles. *Int. J. Nanomed.* **2012**, *7*, 5577−5591.
(34) McCammon, J. A.; Gelin, B. R.; Karplus, M. Dynamics of Folded Proteins. *Nature* **1977**, *267*, 585−590.
(35) Pavan, G. M.; Albertazzi, L.; Danani, A. Ability to Adapt: Different Generations of PAMAM Dendrimers Show Different Behaviors in Binding siRNA. *J. Phys. Chem. B* **2010**, *114*, 2667−2675.
(36) Jensen, L. B.; Mortensen, K.; Pavan, G. M.; Kasimova, M. R.; Jensen, D. K.; Gadzhyeva, V.; Nielsen, H. M.; Foged, C. Molecular Characterization of the Interaction between siRNA and PAMAM G7 Dendrimers by SAXS, ITC, and Molecular Dynamics Simulations. *Biomacromolecules* **2010**, *11*, 3571−3577.
(37) Ouyang, D.; Zhang, H.; Parekh, H. S.; Smith, S. C. Structure and Dynamics of Multiple Cationic Vectors-siRNA Complexation by All-atomic Molecular Dynamics Simulations. *J. Phys. Chem. B* **2010**, *114*, 9231−9237.

DOI: 10.1021/acsami.5b07929
ACS Appl. Mater. Interfaces 2015, 7, 24822−24832